DETERMINATION OF AVERAGED AXISYMMETRIC FLOW SURFACES ACCORDING TO RESULTS OBTAINED BY NUMERICAL SIMULATION OF FLOW IN TURBOMACHINERY

by

Jasmina B. BOGDANOVIĆ-JOVANOVIĆ*, Božidar P. BOGDANOVIĆ, and Dragica R. MILENKOVIĆ

Faculty of Mechanical Engineering, University of Niš, Niš, Serbia

Original scientific paper
DOI: 10.2298/TSCI120426193B

In the increasing need for energy saving worldwide, the designing process of turbomachinery, as an essential part of thermal and hydroenergy systems, goes in the direction of enlarging efficiency. Therefore, the optimization of turbomachinery designing strongly affects the energy efficiency of the entire system. In the designing process of turbomachinery blade profiling, the model of axisymmetric fluid flows is commonly used in technical practice, even though this model suits only the profile cascades with infinite number of infinitely thin blades. The actual flow in turbomachinery profile cascades is not axisymmetric, and it can be fictively derived into the axisymmetric flow by averaging flow parameters in the blade passages according to the circular co-ordinate. Using numerical simulations of flow in turbomachinery runners, its operating parameters can be preliminarily determined. Furthermore, using the numerically obtained flow parameters in the blade passages, averaged axisymmetric flow surfaces in blade profile cascades can also be determined. The method of determination of averaged flow parameters and averaged meridian streamlines is presented in this paper, using the integral continuity equation for averaged flow parameters. With thus obtained results, every designer can be able to compare the obtained averaged flow surfaces with axisymmetric flow surfaces, as well as the specific work of elementary stages, which are used in the procedure of blade designing. Numerical simulations of flow in an exemplary axial flow pump, used as a part of the thermal power plant cooling system, were performed using ANSYS CFX.

Key words: *turbomachinery, averaged flow surface, numerical simulation*

Introduction

Hydraulic turbomachinery is a group of widely used machines, operating independently or as a part of a larger system (such as in thermal power plants or water supply systems), greatly influencing the system energy efficiency. Due to its large use in many different and important energy systems, it is of greatest importance in designing turbomachinery in order to operate with the highest possible efficiency. In other words, the optimal design of turbomachinery affects energy utilization and energy efficiency of the machine and the system in which the machine is built.

* Corresponding author; e-mail: bminja@masfak.ni.ac.rs

Due to complex geometry and calculation procedure, which is partly based on empirical data, the turbomachinery designing procedure usually requires creating several turbomachinery models, in order to conduct laboratory testing of designed operating parameters. This approach requires a lot of time and funds for testing the machine model following every major correction. This paper presents a different approach, based on numerical simulation results, reducing the time and modeling costs, with strong influence on the machine energy efficiency.

In the course of determination of blade profiles for turbomachinery impellers and guide vanes, a model of axisymmetric fluid flows is commonly used, even though this model suits the profile cascades with infinite number of infinitely thin blades [1-4]. By averaging flow velocities according to circular co-ordinate, a flow in the real turbomachinery impeller is derived into a flow in the fictive impeller, which has an infinite number of infinitely thin blades, and where the fictive impeller achieves the same flow declination as the real turbomachine impeller.

Using numerical simulations of flow in a designed turbomachine, its operating parameters can be preliminarily determined, and all flow parameters can be calculated in discrete points inside the flow domain (impeller). According to numerical results, it is possible to determine averaged flow parameters and the geometrical parameters of flow surfaces, which simulate the effect of fictive impeller with infinite number of infinitely thin blades.

In technical practice, it is very important to determine meridian streamlines, by using the integral continuity equation for averaged flow parameters, because the designer can compare these meridian streamlines with chosen meridian streamlines (meridian traces of axisymmetric flow surfaces), which are obtained in the designing process of blade profiling. After determination of meridian streamlines, it is possible to determine the disposition of specific work along meridian streamlines and, therefore, the designer of a turbomachine can compare these specific works with specific works of elementary stages, which are already chosen in the process of blade profiling.

The determination of geometrical parameters of a fictive turbomachinery impeller with an infinite number of infinitely thin blades, and determination of its meridian streamlines is not of crucial importance for turbomachinery designers, therefore, in this paper, this problem will be treated only theoretically.

Numerical simulations of flow in a turbomachine impeller were performed using ANSYS CFX, which can be considered as one of the leading commercial pieces of computational fluid dynamics (CFD) software. This software allows comprehensive post-processing analysis, resulting in calculation of every flow parameter in every discrete point of flow domain.

Numerical simulations of flow in turbomachinery

During the last decade, CFD has become a significant tool for turbomachinery designing and investigation [4, 5]. The development and constant improvement of CFD codes enables obtaining reliable numerical results. The numerical simulations of fluid flow in the turbomachinery were carried out using the ANSYS CFX software. This software includes the so-called turbo-mode, which is a specially designed mode developed for numerical simulation of all kinds of turbomachinery. This is a few steps pre-processing procedure, beginning from defining the geometry model and generating its discretization mesh, *i. e*. creating the boundaries of flow domain. The next pre-processing step implies defining all physical and numerical

parameters, necessary for the numerical procedure, such as fluid property, turbulence models, boundary condition values, and other parameters. After that, the numerical resolving of governing equations (Reynolds averaged Navier-Stokes equations – RANS) has to be performed, using the finite volume method, which allows numerical solving of discretized partial differential equations over entire control volumes of a defined fluid domain. Results of numerical (iterative) procedure are an approximation of each variable value over the entire domain. The results can be calculated and represented in various ways: as calculated value in discrete points in the domain, functional graphs, tables, as visualization of streamlines and vector or scalar fields, *etc*. Thus obtained results representation is very useful in technical practice, and it has become an important part of turbomachinery designing and investigating procedure.

This paper investigates an axial flow pump 2PP30 produced in the Pump factory Jastrebac, Niš, which operates with $n = 1450$ min.$^{-1}$ = 24,167 s^{-1} [5]. This pump is designed to operate as a part of cooling system of thermal power plants, therefore, the pump efficiency influences the energy efficiency of the overall system. The axial pump represents a complex geometry, consisting of a suction bell, a pump impeller (with 4 blades), guide vanes and a diffuser, shown in fig. 1. Considering the pump size and its symmetry, as well as the available computational resources, a numerical simulation of one quarter of the pump (one impeller blade and blade passage around) was performed. The discretization mesh is non-uniform, consisting of approximately 250,000 nodes and 1,000,000 elements. Mesh elements are mainly tetrahedral, with prismatic elements along blades and guide vanes solid surfaces. The pump impeller consists of 55,000 nodes and 261,000 elements, showing that the higher density mesh is created in the area of pump blade and guide vanes, while the suction bell and diffuser have much coarser mesh density.

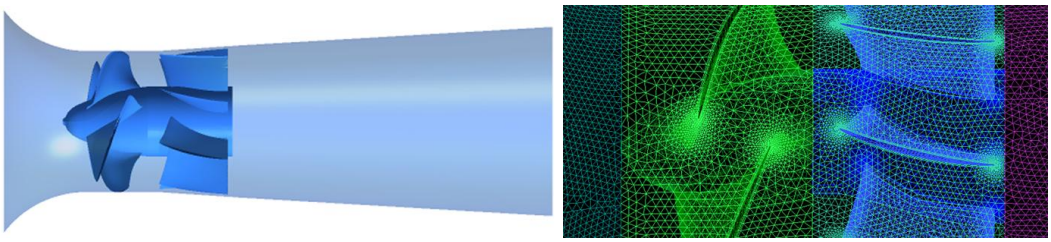

Figure 1. Geometry and discretization mesh of investigated axial flow pump

As it is common practice for numerical simulations of flow in tubomachinery, the standard k-ε turbulence model was used [6, 7].

Interpolation of values from the cell center to the cell faces were accomplished using the high-resolution scheme. Numerical simulations convergence criteria were that the root mean square values of the equation residuals were lower than 10^{-5}.

Numerical simulations for different flow regimes were carried out, and, as a result, the operating characteristics of the investigated axial pump were obtained. For the purpose of numerical model validation, the numerically obtained pump operating diagram was compared to the experimentally obtained operating diagram, as shown in fig. 2. The average result deviation was less than 2.5%. For nominal flow regime (Q = 360 l/s and maximal efficiency), the numerically obtained pump head had a very small deviation of only 1.1%. The maximal deviation of numerical results (4.5%) was acquired for maximal investigated flow rate (Q = 400 l/s) and lowest efficiency.

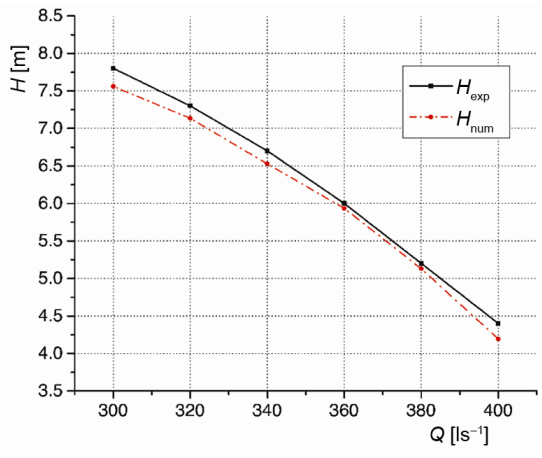

Figure 2. Comparison of operating characteristics obtained experimentally and numerically

For further analysis, the numerical simulation results for nominal (optimal) flow regime, Q = 360 l/s, were used. The flow through the pump impeller, *i. e.* the flow through the one blade passage, was investigated. Numerically calculated values of all flow parameters in discrete points of the impeller enabled obtaining averaged flow surfaces and averaged streamlines in the pump impeller. This could lead pump designers to a clear conclusion if one of the basic designing assumptions was fulfilled, and it is the question of flow surfaces axisymmetry in the pump impeller. If the deviation of actual and axysimmetrical flow surfaces is large, it is the indicator for making necessary changes in pump design.

Averaging of flow parameters according to circular co-ordinate

The flow in the rotating turbomachine impeller was observed in relation to the curvilinear orthogonal co-ordinate system in which the co-ordinate surfaces were: q_3 = const. – meridian planes (planes passing through the axis of the rotating impeller), q_2 = const. – axisymmetric surfaces approximate to averaged flow surfaces and q_1 = const. – axisymmetric surfaces perpendicular to q_3 and q_2 = const.

Since the vectors $[\vec{v}_1, \vec{v}_2]$ direction and $\mathrm{rot}\vec{v}$ direction depended on the co-ordinate system orientation, the right (positive) co-ordinate system was used, therefore, the direction of circumferential co-ordinate $q_3(\vec{e}_3^o)$ did not need to follow the direction of the impeller rotation.

Figure 3 presents characteristic cross-sections of a centrifugal pump, where dashed line in fig. 3(b) shows cross-sections of pump blades, which are designed for impeller rotation in the clockwise direction. Between absolute $(\vec{c})$ and relative $(\vec{w})$ velocity in the rotational impeller, there is a relationship:

$$\vec{c} = \vec{w} + \vec{u} = \vec{w} + \vec{\omega},\vec{r} \tag{1}$$

$$\mathrm{rot}\vec{c} = \mathrm{rot}\vec{w} + 2\vec{\omega}, \quad i.\,e. \quad \mathrm{rot}\vec{w} = \mathrm{rot}\vec{c} - 2\vec{\omega} \tag{1'}$$

Equation (1) yields $c_1 = w_1$ and $c_2 = w_2$, and also:

$$u = -\omega r < 0,\ c_3 = -c_u < 0,\ w_3 = c_3 + \omega r = -c_u + \omega r > 0 \ \text{ for } \vec{e}_3^o = -\vec{u}^o$$

$$u = \omega r > 0,\ c_3 = c_u > 0,\ w_3 = c_3 - \omega r = c_u - \omega r < 0 \ \text{ for } \vec{e}_3^o = \vec{u}^o \tag{1''}$$

According to the cosinus theorem, for velocity triangle, there is a relationship:

$$c^2 = w^2 + \omega^2 r^2 - 2\omega r c_u \quad \Rightarrow \quad w^2 = c^2 - \omega^2 r^2 + 2\omega r c_u$$

$L_1 = \dfrac{\mathrm{d}q_1(q_2)}{\mathrm{d}q_1}$

$L_2 = \dfrac{\mathrm{d}q_2(q_1)}{\mathrm{d}q_2}$

$L_3 = \dfrac{\mathrm{d}q_3(r)}{\mathrm{d}q_3}$

$q_3 = r_o\varphi$

$L_3 = r/r_o$

$q_3(r) = L_3 q_3 = r\varphi$

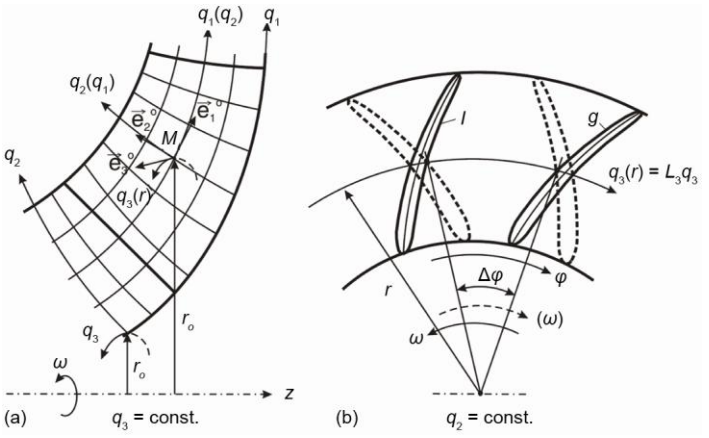

Figure 3. Cross-sections of centrifugal pump impeller

Scalar flow parameters, such as pressure $p(q_1,q_2,q_3)$ and flow velocity components $w_j(q_1,q_2,q_3), j=1,2,3,$ $c_j(q_1,q_2,q_3), j=1,2,3,$ and any other scalar function $f(q_1,q_2,q_3)$ can be averaged according to circumferential co-ordinate $q_3 = r_o\varphi$.

Denoting "a" and "b" surfaces of the two next blades, which create a blade passage, the averaging interval is $\Delta q_3 = q_{3b}(q_1,q_2) - q_{3a}(q_1,q_2)$, where $q_{3b}(q_1,q_2)$ and $q_{3a}(q_1,q_2)$ are the equations of blade surfaces in the blade passage.

The averaging of a scalar function $f(q_1,q_2,q_3)$ according to circumferential co-ordinate q_3 can be obtained using formula:

$$\overline{f}\ q_1,q_2\ = \frac{1}{\Delta q_3}\int_{q_{3a}(q_1,q_2)}^{q_{3b}(q_1,q_2)} f\ q_1,q_2,q_3\ \mathrm{d}q_3, \quad \text{where} \quad \Delta q_3 = \Delta q_3(q_1,q_2) \tag{2}$$

Circumferential co-ordinate line $q_3 = L_3 q_3 = r\varphi$ passes through the point M(q_1,q_2) in meridian cross-section of pump impeller (fig. 3), where $r = r(q_1,q_2)$. Since $\Delta q_3 = \Delta q_3(r)/L_3$ and $\mathrm{d}q_3 = \mathrm{d}q_3(r)/L_3$, eq. (2) can be transformed into the form:

$$\overline{f}\ q_1,q_2\ = \frac{1}{\Delta q_3}\int_{q_{3a}(r)}^{q_{3b}(r)} f\ q_1,q_2,q_3(r)\ \mathrm{d}q_3(r) = \frac{1}{\Delta\varphi(r)}\int_{\varphi_a(r)}^{\varphi_b(r)} f\ q_1,q_2,\varphi(r)\ \mathrm{d}\varphi(r) \tag{2'}$$

where $r = r(q_1,q_2)$, $\Delta q_3(r) = r\Delta\varphi(r)$, and $\Delta\varphi(r) = \varphi_b(r) - \varphi_a(r)$.

Denoting "l" as the suction and "g" as the pressure side of the blade, as it is shown in fig. 3, notation "a" and "b", used in eqs. (2) and (2'), can be replaced with indexes "l" and "g", and, therefore: $a = l, b = g$ for $\vec{e} = -\vec{u}$, respectively $a = g, b = l$ for $\vec{e} = \vec{u}$.

Averaging interval in eq. (2') is a circular arc in the blade passage, thus the averaging of scalar values $f(q_1,q_2,q_3)$ is performed according to its function distribution over a circular arc. For this reasons, the eq. (2') can be used for determination of scalar flow values (such as $\overline{p}(q_1,q_2)$, $\overline{w}_j(q_1,q_2)$, $\overline{c}_j(q_1,q_2), j=1,2,3$), taking into account numerically obtained distribution of these values over circular arcs in the blade passage. If numerical results are obtained for large number of points, the integral in eq. (2') can be calculated with satisfying accuracy, using the trapezoidal rule.

From the averaging formula (2) the following expressions can be derived:

$$\left(\overline{\frac{\partial f}{\partial q_3}}\right) = \frac{1}{\Delta q_3}\Delta f, \quad \text{where} \quad \Delta f = f_{\mathrm{b}}(q_1, q_2) - f_{\mathrm{a}}(q_1, q_2) \tag{3}$$

$$\left(\overline{\frac{\partial f}{\partial q_{1,2}}}\right) = \frac{1}{\Delta q_3}\frac{\partial\, \Delta q_3\, \overline{f}}{\partial q_{1,2}} - \frac{1}{\Delta q_3}\Delta\left(f\frac{\partial q_3}{\partial q_{1,2}}\right), \quad \text{where} \quad \Delta\left(f\frac{\partial q_3}{\partial q_{1,2}}\right) = \left(f\frac{\partial q_3}{\partial q_{1,2}}\right)_{\mathrm{b}} - \left(f\frac{\partial q_3}{\partial q_{1,2}}\right)_{\mathrm{a}} \tag{4}$$

Equations (3) and (4) are the most important for averaging flow equations. Figure 4 presents cross-sections of an axial turbo pump and surfaces q_3 = const., q_2 = const. and q_1 = const. Inclination angles of blade profiles are denoted with $\beta_{\mathrm{a,b}}$ and $\alpha_{\mathrm{a,b}}$, and they are measured, as it is common for turbomachinery, according to negative direction of circumferential velocity. Components of external perpendiculars on boundary blade surfaces in the blade passage ($n_{1\mathrm{a,b}}$, $n_{2\mathrm{a,b}}$, $n_{3\mathrm{a,b}}$) are also shown in fig. 4.

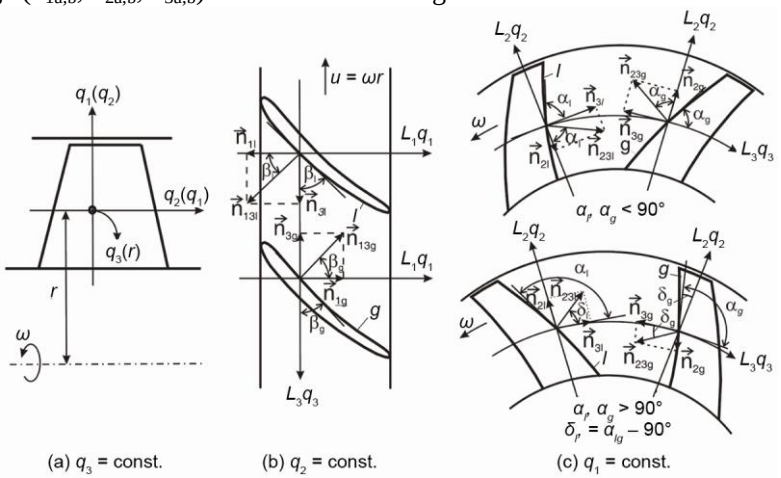

Figure 4. Cross-sections of axial pump impeller

Figure 4 shows the following expressions, for $\vec{e}_3^{\,o} = -\vec{u}^{\,o}\,(a = l,\, b = g)$:

$$\left(\frac{dq_3}{dq_1}\right)_{\mathrm{a,b}} = \frac{L_1}{L_3}\mathrm{ctg}\beta_{\mathrm{a,b}} = -\frac{L_1}{L_3}\left(\frac{n_1}{n_3}\right)_{\mathrm{a,b}}, \quad \left(\frac{dq_3}{dq_2}\right)_{\mathrm{a,b}} = \frac{L_2}{L_3}\mathrm{ctg}\alpha_{\mathrm{a,b}} = -\frac{L_2}{L_3}\left(\frac{n_2}{n_3}\right)_{\mathrm{a,b}} \tag{5}$$

and

$$\left(\frac{\vec{n}}{n_3}\right)_{\mathrm{a,b}} = -\mathrm{ctg}\beta_{\mathrm{a,b}}\vec{e}_1^{\,o} - \mathrm{ctg}\alpha_{\mathrm{a,b}}\vec{e}_2^{\,o} + \vec{e}_3^{\,o} \tag{5'}$$

If $\vec{e}_3^{\,o} = -\vec{u}^{\,o}\,(a = g,\, b = 1)$, the previous expressions become:

$$\left(\frac{dq_3}{dq_1}\right)_{\mathrm{a,b}} = -\frac{L_1}{L_3}\mathrm{ctg}\beta_{\mathrm{a,b}} = -\frac{L_1}{L_3}\left(\frac{n_1}{n_3}\right)_{\mathrm{a,b}}, \quad \left(\frac{dq_3}{dq_2}\right)_{\mathrm{a,b}} = -\frac{L_2}{L_3}\mathrm{ctg}\alpha_{\mathrm{a,b}} = -\frac{L_2}{L_3}\left(\frac{n_2}{n_3}\right)_{\mathrm{a,b}} \tag{6}$$

and

$$\left(\frac{\vec{\mathrm{n}}}{n_3}\right)_{\mathrm{a,b}} = \mathrm{ctg}\beta_{\mathrm{a,b}}\vec{\mathrm{e}}_1^{\,\mathrm{o}} + \mathrm{ctg}\alpha_{\mathrm{a,b}}\vec{\mathrm{e}}_2^{\,\mathrm{o}} + \vec{\mathrm{e}}_3^{\,\mathrm{o}} \tag{6'}$$

The difference between formulas (5) and (6) appears due to the different sign of value $(n_3)_{\mathrm{a,b}}$ in the co-ordinate system where $\vec{\mathrm{e}}_3^{\,\mathrm{o}} = -\vec{\mathrm{u}}^{\,\mathrm{o}}$ or $\vec{\mathrm{e}}_3^{\,\mathrm{o}} = \vec{\mathrm{u}}^{\,\mathrm{o}}$. Note that blade profile shapes in these cases are not the same (fig. 4b). Due to eq. (5) and eq. (6), eq. (4) can be derived into the form:

$$\left(\overline{\frac{\partial f}{\partial q_{1,2}}}\right) = \frac{1}{\Delta q_3}\frac{\partial\ \Delta q_3 \overline{f}}{\partial q_{1,2}} + \frac{1}{\Delta q_3}\frac{L_{1,2}}{L_3}\Delta\left(f\frac{n_{1,2}}{n_3}\right) \tag{7}$$

where $\Delta\left(f\dfrac{n_{1,2}}{n_3}\right) = \left(f\dfrac{n_{1,2}}{n_3}\right)_b - \left(f\dfrac{n_{1,2}}{n_3}\right)_a$, for $\mathrm{M}(q_1, q_2)$.

According to eq. (3) and eq. (7) and formulas for $\mathrm{grad}\, f(q_1, q_2, q_3)$, $\mathrm{div}\vec{\mathrm{v}}(q_1, q_2, q_3)$ and $\mathrm{rot}\vec{\mathrm{v}}(q_1, q_2, q_3)$, averaged values of these functions are:

$$\left.\begin{aligned}
\overline{\mathrm{grad}f} &= \frac{1}{\Delta q_3}\cdot\mathrm{grad}\ \Delta q_3\cdot\overline{f}\ + \frac{1}{L_3\Delta q_3}\Delta\left(f\frac{\vec{n}}{n_3}\right) = \mathrm{grad}\overline{f} + \frac{1}{L_3\Delta q_3}\Delta\left(f'\frac{\vec{n}}{n_3}\right)\\
\overline{\mathrm{div}\vec{v}} &= \frac{1}{\Delta q_3}\mathrm{div}\ \Delta q_3,\overline{\vec{v}}\ + \frac{1}{L_3\Delta q_3}\Delta\left(\frac{\vec{n}}{n_3},\vec{v}\right) = \mathrm{div}\overline{\vec{v}} + \frac{1}{L_3\Delta q_3}\Delta\left(\frac{\vec{n}}{n_3},\vec{v}'\right)\\
\overline{\mathrm{rot}\vec{v}} &= \frac{1}{\Delta q_3}\mathrm{rot}\ \Delta q_3,\overline{\vec{v}}\ + \frac{1}{L_3\Delta q_3}\Delta\left[\frac{\vec{n}}{n_3},\vec{v}\right] = \mathrm{rot}\overline{\vec{v}} + \frac{1}{L_3\Delta q_3}\Delta\left[\frac{\vec{n}}{n_3},\vec{v}'\right]
\end{aligned}\right\} \tag{8}$$

where $f' = f - \overline{f}$ and $\vec{\mathrm{v}}' = \vec{\mathrm{v}} - \overline{\vec{\mathrm{v}}}$, and, for $\mathrm{M}(q_1, q_2)$, operator Δ denotes the function difference in boundary points of the averaging interval in blade passage (points $b(q_1, q_2, q_{3.\mathrm{b}})$ and $a(q_1, q_2, q_{3.\mathrm{a}})$ on the blade surfaces in the blade passage).

Since $f = \overline{f} + f'$ and $\vec{\mathrm{v}} = \overline{\vec{\mathrm{v}}} + \vec{\mathrm{v}}'$, also apply $\overline{\mathrm{grad}f} = \mathrm{grad}\overline{f} + \overline{\mathrm{grad}f'}$, $\overline{\mathrm{div}\vec{\mathrm{v}}} = \mathrm{div}\overline{\vec{\mathrm{v}}} + \overline{\mathrm{div}\vec{\mathrm{v}}'}$ and $\overline{\mathrm{rot}\vec{\mathrm{v}}} = \mathrm{rot}\overline{\vec{\mathrm{v}}} + \overline{\mathrm{rot}\vec{\mathrm{v}}'}$, therefore, according to eq. (8):

$$\overline{\mathrm{grad}f'} = \frac{1}{L_3\Delta q_3}\Delta\left(f',\frac{\vec{\mathrm{n}}}{n_3}\right),\ \overline{\mathrm{div}\vec{\mathrm{v}}'} = \frac{1}{L_3\Delta q_3}\Delta\left(\frac{\vec{\mathrm{n}}}{n_3},\vec{\mathrm{v}}'\right),\ \overline{\mathrm{rot}\vec{\mathrm{v}}'} = \frac{1}{L_3\Delta q_3}\Delta\left[\frac{\vec{\mathrm{n}}}{n_3},\vec{\mathrm{v}}'\right] \tag{8'}$$

Values $\overline{\mathrm{grad}f'}$, $\overline{\mathrm{div}\vec{\mathrm{v}}'}$ and $\overline{\mathrm{rot}\vec{\mathrm{v}}'}$ are caused by blade effect on averaged flow. In the flow space without blades, these values are equal to zero.

Averaging of flow equations

Flow in the hydraulic turbomachinery impellers is extremely turbulent, therefore, kinematic characteristics of flow obtained by calculations for inviscous fluids are in good agreement with kinematic characteristics of real mean (time averaged) turbulent flow. Nominal operating regimes (operating with maximal efficiency), or regimes close to nominal, are considered here.

For this reason, not just for the methodological purpose, to describe the steady flow in hydraulic turbomachinery, the flow equation for inviscous fluid joins the continuity equation ($\mathrm{div}\vec{w}=0$), and if the gravitational influence is neglected, it can be written in the form:

$$\vec{\mathrm{w}},\mathrm{rot}\vec{\mathrm{c}} = \mathrm{grad}E \tag{9}$$

where: $\mathrm{rot}\vec{\mathrm{c}} = \mathrm{rot}\vec{\mathrm{w}} - 2\vec{\omega}$ and E is the Bernoulli's integral for relative fluid flow in rotational space of turbomachinery,

$$E = \frac{p}{\rho} + \frac{w^2}{2} - \frac{(r\omega)^2}{2}, \quad E = E(q_1, q_2, q_3) \tag{9'}$$

In the turbomachine impeller inlet, which is placed in front of the blade cascade, there is a relationship between Bernoulli's integrals for relative (E_o) and absolute (G_o) fluid flow:

$$E_\mathrm{o} = G_\mathrm{o} - \omega(rc_\mathrm{u})_\mathrm{o}, \quad G_\mathrm{o} = \frac{p_\mathrm{o}}{\rho} + \frac{c_\mathrm{o}^2}{2}$$

where notation "o" defines the flow and geometrical parameters on the control surface that defines the inlet area into the operating space of the turbomachine.

In the circular co-ordinate averaged continuity equation $\overline{\mathrm{div}\vec{\mathrm{w}}} = 0$, according to eq. (8), can be written as follows:

$$\mathrm{div}\ \Delta q_3, \bar{\vec{\mathrm{w}}} + \frac{1}{L_3}\Delta\left(\frac{\vec{\mathrm{n}}}{n_3}, \vec{\mathrm{w}}\right) = 0 \tag{9}$$

According to inviscous fluid flow model, blade surfaces are flow surfaces ($\vec{\mathrm{n}} \perp \vec{\mathrm{w}}$), therefore, the second element on the left side of equation is equal to zero, and averaged equation becomes:

$$\mathrm{div}\ \Delta q_3, \bar{\vec{\mathrm{w}}} = 0, \quad i.e. \quad \frac{\partial}{\partial q_1} L_2 L_3 \Delta q_3 \bar{w}_1 = -\frac{\partial}{\partial q_2} L_3 L_1 \Delta q_3 \bar{w}_2 \tag{11}$$

where $L_1 = L_1(q_1, q_2)$, $L_2 = L_2(q_1, q_2)$, and $L_3 = r(q_1, q_2)/r_\mathrm{o}$ are Lamé's coefficients.

Multiplying the eq. (11) with $2\pi/\tau$ ($\tau = 2\pi/z_1$ – angular blade pitch, z_1 –number of blades), and applying $\Delta q_3 = r_\mathrm{o}\Delta\varphi_3$, the following equation is obtained:

$$\frac{\partial}{\partial q_1} 2\pi r_o k L_3 L_2 \bar{w}_1 = -\frac{\partial}{\partial q_2} 2\pi r_o k L_3 L_1 \bar{w}_2 \tag{11'}$$

where $k = \Delta\varphi/\tau = (z_1\Delta\varphi\ [\mathrm{rad}])/2\pi$ is the blockage factor (coefficient of flow cross-section reduction) due to actual thickness of the impeller blades [$\Delta\varphi = \Delta\varphi(q_1, q_2)$, $k = k(q_1, q_2)$].

The eq. (11') represents necessary and sufficient condition for existence of meridian stream function, $\psi_\mathrm{m} = \psi_\mathrm{m}(q_1, q_2)$ – stream function of averaged meridian velocity $\bar{\vec{\mathrm{w}}}_\mathrm{m} = \bar{w}_1\vec{\mathrm{e}}_1^{\,o} + \bar{w}_2\vec{\mathrm{e}}_2^{\,o}$. Meridian streamlines averaged in the circular co-ordinate represent traces of section between flow surface S_m and meridian plane (q_3 = const.). According to eq. (11'), it can be written as:

$$\frac{\partial \bar{\psi}_{\mathrm{m}}}{\partial q_1} = -2\pi r_o k L_3 L_2 \bar{w}_2 \quad \text{and} \quad \frac{\partial \bar{\psi}_{\mathrm{m}}}{\partial q_2} = 2\pi r_o k L_3 L_1 \bar{w}_1 \tag{12}$$

For the known field of averaged meridian velocities $\bar{w}_1(q_1,q_2)$ and $\bar{w}_2(q_1,q_2)$, and known function of cross-section reduced coefficient due to actual thickness of the blades $k(q_1,q_2)$, using the equation (12), the meridian stream function $\psi_{\mathrm{m}}(q_1,q_2)$ can be determined, *i. e.* meridian streamlines $\psi_{\mathrm{m}}(q_1,q_2) = \text{const.}$, which represent traces of the sections between averaged axisymmetric flow surfaces and meridian planes. It can be demonstrated easily that $\mathrm{d}\psi_{\mathrm{m}} = \mathrm{d}Q$, and the flow rate through the randomly selected axysimmetrical cross-section, where meridian trace is a line A-B, shown in fig. 5, can be calculated as $Q = \psi_{\mathrm{mB}} - \psi_{\mathrm{mA}}$.

Averaged continuity eq. (10) is valid for primary (mean) turbulent flow, but the second element of this equation can be neglected only in cases of very thin boundary layer in the rotational impeller (if results are obtained using the model of inviscous fluid, they show very good agreement with turbulent fluid flow). Actual flows in rotational impeller of hydraulic turbomachinery are highly turbulent, but followed by smaller or larger separations of boundary layers from the blade surfaces, or other solid surfaces. In such cases, the second element of averaged continuity eq. (10) cannot be neglected, and eq. (12) cannot be used for determination of meridian streamline. Meridian streamlines shall be determined by the condition of equal flow rate passing between axisymmetric flow surface and hub surface.

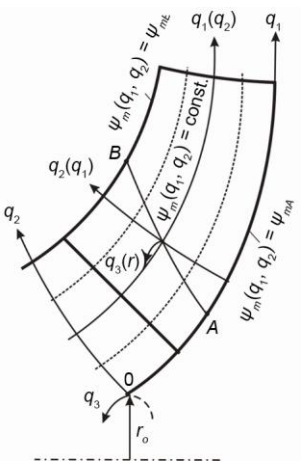

Figure 5. Meridian cross-section

Since, $\vec{w} = \bar{\vec{w}} + \vec{w}'$ and $\mathrm{rot}\vec{c} = \overline{\mathrm{rot}\vec{c}} + (\mathrm{rot}\vec{c})'$, the averaged equation of relative flow in turbomachinery impeller (9) can be written in the form:

$$\left[\bar{\vec{w}}, \overline{\mathrm{rot}\vec{c}}\right] + \overline{\vec{w}', (\mathrm{rot}\vec{c})'} = \overline{\mathrm{grad}E} \tag{13}$$

Given the formulas (8) for $\overline{\mathrm{rot}\vec{c}}$ and $\overline{\mathrm{grad}E}$, and the fact that $\vec{c}' = \vec{w}'$, $(\mathrm{rot}\vec{c})' = \mathrm{rot}\vec{c}' - \overline{\mathrm{rot}\vec{c}'} = \mathrm{rot}\vec{w}' - \overline{\mathrm{rot}\vec{w}'}$, , the previus equation becomes:

$$\left[\bar{\vec{w}}, \mathrm{rot}\bar{\vec{c}}\right] + \vec{F}^{\,1} + \vec{F}^{\,2} + \vec{F}^{\,3} = \mathrm{grad}\bar{E} \tag{13'}$$

where

$$\vec{F}^{\,1} = \left[\bar{\vec{w}}, \frac{1}{L_3 \Delta q_3} \Delta\left(\frac{\vec{n}}{n_3}, \vec{w}'\right)\right], \quad \vec{F}^{\,2} = \frac{1}{L_3 \Delta q_3} \Delta\left(E', \frac{\vec{n}}{n_3}\right), \quad \vec{F}^{\,2} = \overline{\vec{w}', \mathrm{rot}\vec{w}'} \tag{13''}$$

Forces $\vec{F}^{\,(1)}$, $\vec{F}^{\,(2)}$, $\vec{F}^{\,(3)}$ are results of averaging, and can be treated as mass force of blades acting on the averaged flow. The force $\vec{F}^{\,(3)}$ is much smaller than $\vec{F}^{\,(1)}$ [8]. If components of velocity $\vec{w}$ changes linearly over the circumferential co-ordinate q_3, it can be easily proven (for radial and axial turbo pumps) that components of the force $\vec{F}^{\,(3)}$ are many times smaller than components of the force $\vec{F}^{\,(1)}$, thus the effect of the force $\vec{F}^{\,(3)}$ can be disregarded.

For inviscous flow, $\vec{F}^{\,(3)} = 0$, and according to ref. [8], this force can also be disregarded. Since forces $\vec{F}^{\,(1)}$ and $\vec{F}^{\,(2)}$ are determined according to numerical simulations results,

which take into account the flow viscosity, the force $\vec{F}^{(2)}$ may not be negligible compared to $\vec{F}^{(1)}$. Thus, in the following text applies: $\vec{F} = \vec{F}^{(1)} + \vec{F}^{(2)}$, and the eq. (13) becomes:

$$\left[\bar{\vec{w}}, \mathrm{rot}\bar{\vec{c}}\right] + \vec{F} = \mathrm{grad}\bar{E} \tag{14}$$

According to eq. (13'), components of force $\vec{F}$, are:

$$F_1 = F_1^{\,1} + F_1^{\,2}\,, \quad F_2 = F_2^{\,1} + F_2^{\,2} \quad \text{and} \quad F_3 = F_3^{\,1} + F_3^{\,2} \tag{15}$$

where

$$\left.\begin{aligned} F_1^{\,1} &= \mp\frac{1}{L_3\Delta q_3}\left[\Delta\ \bar{w}_2 w_2' + \bar{w}_3 w_3'\ \ \mathrm{ctg}\beta \pm \bar{w}_2\Delta\ \ w_1'\mathrm{ctg}\alpha\ - \bar{w}_3\Delta w_1'\right] \\ F_2^{\,1} &= \mp\frac{1}{L_3\Delta q_3}\left[\Delta\ \bar{w}_3 w_3' + \bar{w}_1 w_1'\ \ \mathrm{ctg}\alpha \pm \bar{w}_1\Delta\ \ w_2'\mathrm{ctg}\beta\ - \bar{w}_3\Delta w_2'\right] \\ F_3^{\,1} &= \pm\frac{\bar{w}_1}{L_3\Delta q_3}\left[\Delta\ \bar{w}_3\mathrm{ctg}\beta\ \pm \bar{w}_2\Delta\ \ w_3'\mathrm{ctg}\alpha\ + \bar{w}_1\Delta w_1' + \bar{w}_2\Delta w_2'\right] \end{aligned}\right\} \tag{15'}$$

and

$$F_3^{\,2} = \pm\frac{1}{L_3\Delta q_3}\Delta\ E', \mathrm{ctg}\beta\ ,\ F_1^{\,2} = \pm\frac{1}{L_3\Delta q_3}\Delta\ E', \mathrm{ctg}\alpha\ ,\ \text{and}\ \ F_2^{\,2} = -\frac{1}{L_3\Delta q_3}\Delta E \tag{15''}$$

Flow surfaces $\bar{S}_1$, perpendicular to the force field $\vec{F}$, simulate the effect of infinite number of infinitely thin blades. Vector $\vec{n}_{sr}$ normal to the surface $\bar{S}_1$ are collinear to the force vector $\vec{F}$, therefore: $(n_1/n_3)_{sr} = F_1/F_3$ and $(n_2/n_3)_{sr} = F_2/F_3$. Denoting $q_{3_{sr}}(q_1, q_2)$ the equation of flow surface $\bar{S}_1$, also β_{sr} and α_{sr} its angles, it can be assumed, the same as for real blades, that relations (5) and (6) exist. In this case:

$$\left(\frac{n_1}{n_3}\right)_{sr} = \frac{F_1}{F_3} = \mp\mathrm{ctg}\beta_{sr} = \mp\frac{L_3}{L_1}\frac{\partial q_{3_{sr}}}{\partial q_1} \quad \text{and} \quad \left(\frac{n_2}{n_3}\right)_{sr} = \frac{F_2}{F_3} = \mp\mathrm{ctg}\alpha_{sr} = \mp\frac{L_3}{L_2}\frac{\partial q_{3_{sr}}}{\partial q_2} \tag{16}$$

where sign "– " corresponds to $\vec{e}_3^{\,o} = -\vec{u}^{\,o}$, and sign "+" to $\vec{e}_3^{\,o} = \vec{u}^{\,o}$.

According to the model of inviscous flow $\vec{F} = \vec{F}^{\,1}$, and considering the formula (15') for $\vec{F}^{\,1}$, one can conclude that mass forces act perpendicular to the averaged relative velocities $\bar{\vec{w}}$, $(\vec{w}, \vec{F}^{(1)}) = 0$.

General equation of averaged axisymmetric flow in turbomachinery impeller

For inviscous fluids, $\bar{E}\ \bar{\psi} = \mathrm{const.} = \bar{E}_o\ \bar{\psi}$, where index "o" denotes the inlet control flow surface, and $\bar{\psi}$ represents the meridian stremline of averaged fluid flow. In real (viscous) fluids, there are mechanical flow energy losses, thus:

$$\bar{E}\ \bar{\psi} = \bar{E}_o\ \bar{\psi} - \Delta\bar{E}_g\ \bar{\psi} = \bar{G}_o\ \bar{\psi} - \omega\ r\bar{c}_{u\ o}\ \bar{\psi} - \Delta\bar{E}_g\ \bar{\psi} \tag{17}$$

where $\Delta E_g\ \bar{\psi}$ represents the averaged mechanical flow energy loses, from the inlet control surface "o", in the impeller inlet, to the arbitrary circular cross-section on the averaged flow

surface, whose meridian trace is the line $\bar{\psi}(q_1,q_2)=\text{const.}$ $\bar{G}_o(\bar{\psi})$ is the Bernoulli's integral for averaged absolute flow ($\bar{G}_o(\bar{\psi})=\bar{p}_o/\rho+\bar{c}_o^2/2$, where $\bar{c}_u=-\bar{c}_3$ for $\vec{e}_3^o=-\vec{u}^o$ or $\bar{c}_u=\bar{c}_3$ for $\vec{e}_3^o=\vec{u}^o$.

Starting from the averaged flow eq. (14), for inviscous fluid ($\vec{F}=\vec{F}^{(3)}$), and taking into account the influence of viscosity using the eq. (17) [7], the general equation of averaged flow in turbomachinery impellers is derived into the form:

$$\frac{1}{rL_2}\frac{\partial\, r\bar{c}_u}{\partial q_2}\text{ctg}\beta_{sr}-\frac{1}{rL_1}\frac{\partial\, r\bar{c}_u}{\partial q_1}\text{ctg}\alpha_{sr}+\frac{1}{L_1L_2}\left[\frac{\partial\, L_2\bar{c}_2}{\partial q_1}-\frac{\partial\, L_1\bar{c}_1}{\partial q_2}\right]+$$
$$+\frac{1}{\bar{c}_1L_2}\frac{\partial\bar{G}_o\;\bar{\psi}}{\partial q_2}-\frac{\omega}{\bar{c}_1L_2}\frac{\partial\, r\bar{c}_u\;\bar{\psi}}{\partial q_2}-\frac{\partial\,\Delta\bar{E}_g\;\bar{\psi}}{\partial q_2}=0 \tag{18}$$

where $\bar{c}_u=-\bar{c}_3$ for $\vec{e}_3^o=-\vec{u}^o$ or $\bar{c}_u=\bar{c}_3$ for $\vec{e}_3^o=\vec{u}^o$.

Determination of angles β_{sr} and α_{sr} using the eq. (16), additionally include the effect or viscose friction in the eq. (18).

Since, $\bar{c}_1=\bar{w}_1$, $\bar{c}_2=\bar{w}_2$ and $\bar{c}_u=-\bar{c}_3=-\bar{w}_3+\omega r$ for $\vec{e}_3^o=-\vec{u}^o$ and $\bar{c}_u=\bar{c}_3=$ $=\bar{w}_3+\omega r$ for $\vec{e}_3^o=\vec{u}^o$, the general equation of relative flow (18) can be derived into the form which depends on averaged relative flow velocities.

If $S_1=q_1(q_2)$ represents meridian streamlines of averaged flow, and S_2 are perpendicular to the S_1 ($\text{d}S_1=L_1\text{d}q_1$, $\text{d}S_2=L_2\text{d}q_2$), with the fact that $\bar{c}_1=\bar{c}_m$ and $\bar{c}_2=0$, the eq. (18) derives into the form:

$$\frac{\partial\bar{c}_m}{\partial S_2}=K_1\bar{c}_m+\frac{1}{r}\frac{\partial(r\bar{c}_u)}{\partial S_2}\text{ctg}\beta_{sr}-\frac{1}{r}\frac{\partial(r\bar{c}_u)}{\partial S_1}\text{ctg}\alpha_{sr}+$$
$$+\frac{1}{\bar{c}_m}\left[\frac{\partial\bar{G}_o(\bar{\psi})}{\partial S_2}-\omega\frac{\partial\, r\bar{c}_u\;(\bar{\psi})}{\partial S_2}-\frac{\partial\,\Delta\bar{E}_g(\bar{\psi})}{\partial S_2}\right] \tag{19}$$

where $K_1\,(=1/\text{R}_1)$ is the curvature of streamline S_1, and $K_2\,(=1/\text{R}_2)$ is the curvature of streamline S_2.

For obtaining the meridian velocity $\bar{c}_m$ disposition along a line l, which in general case deviates from the co-ordinate line S_2, the differential eq. (19) derives into a form that is more convenient. If δ is an angle between normal vector $\vec{n}_1$ on the line l and tangent $\vec{e}_1^o$ on the co-ordinate line S_1, as shown in fig. 6, it can be written: $\sin\delta=$ $=\text{d}S_1/\text{d}l$, $\cos\delta=\text{d}S_2/\text{d}l$, $\text{d}/\text{d}l=\sin\delta\,(\partial/\partial S_1)+$ $+\cos\delta\,(\partial/\partial S_2)$. Respectively:

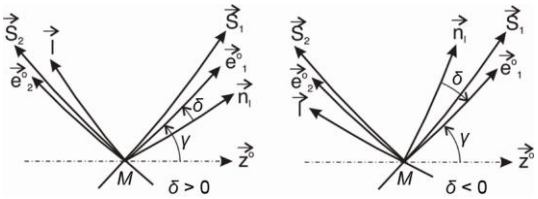

Figure 6. Vectors and angles

$$\frac{\partial}{\partial S_2}=\frac{1}{\cos\delta}\frac{\text{d}}{\text{d}l}-\text{tg}\delta\frac{\partial}{\partial S_1} \tag{20}$$

Using relation (20) and other relations as well, differential eq. (19) derives into the form [8]:

$$\frac{\partial \overline{c}_{\mathrm{m}}}{\partial t}+\overline{c}_{\mathrm{m}}\left[\frac{1}{r}\cos^2\beta_{\mathrm{sr}}\cos\delta\cos\gamma-K_1\sin^2\beta_{\mathrm{sr}}\cos\delta+\sin\delta\left(K_2+\frac{\sin\gamma}{r}+\frac{1}{k}\frac{\partial k}{\partial S_1}\right)+\right.$$

$$\left.+\mathrm{ctg}\beta_{\mathrm{sr}}\mathrm{ctg}\alpha_{\mathrm{sr}}\sin^2\beta_{\mathrm{sr}}\cos\delta\left(K_2+\frac{1}{k}\frac{\partial k}{\partial S_1}\right)-\mathrm{ctg}\beta_{\mathrm{sr}}\frac{\mathrm{d}\beta_{\mathrm{sr}}}{\mathrm{d}l}+\sin\delta\mathrm{ctg}\beta_{\mathrm{sr}}+\cos\delta\mathrm{ctg}\alpha_{\mathrm{sr}}\frac{\mathrm{d}\beta_{\mathrm{sr}}}{\mathrm{d}S_1}\right]=$$

$$=\sin^2\beta_{\mathrm{sr}}\cos\delta\left\{2\omega\left[\cos\gamma\mathrm{ctg}\beta_{\mathrm{sr}}-\sin\gamma\mathrm{ctg}\alpha_{\mathrm{sr}}-\pi L_3 k\frac{\partial\ r\overline{c}_{\mathrm{u}}\ \overline{\psi}}{\partial\overline{\psi}}\right]+\right.$$

$$\left.+2\pi L_3 k\left[\frac{\mathrm{d}\overline{G}_{\mathrm{o}}\ \overline{\psi}}{\mathrm{d}\overline{\psi}}-\frac{\mathrm{d}\ \Delta\overline{E}_{\mathrm{g}}\ \overline{\psi}}{\mathrm{d}\overline{\psi}}\right]\right\}$$

For each intersection meridian control line l: $\beta_{\mathrm{sr}}=\beta_{\mathrm{sr}}\ l\ ,\ \alpha_{\mathrm{sr}}=\alpha_{\mathrm{sr}}\ l\ ,\ K_1=K_1\ l\ ,\ K_2=K_2\ l\ ,\ k=k\ l\ ,\ \delta=\delta\ l\ ,\ \gamma=\gamma\ l\ ,\ \partial k/\partial S_1=f\ l$ *etc.*, therefore, the previous equation becomes:

$$\frac{\partial \overline{c}_{\mathrm{m}}}{\partial l}+M\ l\ \overline{c}_{\mathrm{m}}=N\ l \tag{21}$$

Equation (21) is a quasi-linear differential equation, because the element $N(l)$ contains non-linear elements of the derivative $\partial/\partial\overline{\psi}$. Thus, the differential equation needs to be solved iteratively, and in each iterative step meridian streamlines are determined according to velocity distribution $\overline{c}_{\mathrm{m}}\ l$ along the arbitrarily chosen control lines l.

In order to minimize the number of iterative steps for determination of meridian streamlines in the fictive impeller with an infinite number of infinitively thin blades, in the first iterative step, streamlines are determined using the integral continuity equation.

Determination of points of averaged flow parameters

In the flow domain of the impeller, the series of control sections of meridian lines are arbitrarily set. In fig. 7 these lines are denoted as l_{a}, l_{b}, l_{c}, l_{d}, and l_{e}. Along each of these lines the series of calculating points (0, 1, 2,…, n) is placed, in which, according to the numerical simulation, averaged flow parameters in the impeller are calculated.

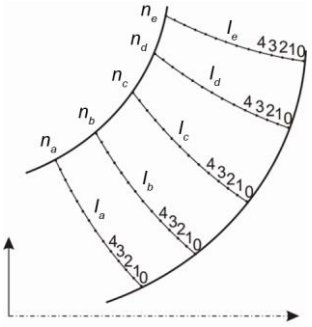

Figure 7. Meridian lines control sections

In order to calculate averaged flow parameters, using equation (2'), in each calculated meridian point of blade passage, a circular arc is withdrawn: $\Delta q_3(r)=r\Delta\varphi$, where $\Delta\varphi=2\pi/z_1$. Along all circular arcs, the discrete points, in which flow parameters are numerically obtained, are placed densely.

In this procedure, it is very important to determined points in the pressure and suction blade side as accurately as possible.

Numerical simulation results are calculated points in every chosen discrete point, and these parameters are: velocities w_{r}, w_{z}, w_{φ}, c_{r}, c_{z}, c_{φ}, w^2, c^2, static pressure p, and total pressure $p_{\mathrm{t}}=p+\rho c^2/2$. According to formula (2'), all these parameters have to be averaged in meridian calculating points.

Determination of meridian streamlines of averaged flow using the integral continuity equation

The volume flow rate through the axisymmetric flow surface, where the meridian trace is a line *l*, can be calculated using the formula:

$$Q_l = 2\pi\left[\int_{r_o(l)}^{r_n(l)} kc_z r\mathrm{d}r - \int_{z_o(r_o)}^{z_n(r_n)} kc_r r\mathrm{d}z\right] \tag{22}$$

and the volume flow rate through a part of this surface, from the calculating point 0 to the calculating point *j* (*j* = 1,2,3,…,n), can be determined using the formula:

$$Q_{l\ \ \mathrm{j}} = 2\pi\left[\int_{r_o(l)}^{r_j(l)} kc_z r\mathrm{d}r - \int_{z_o(r_o)}^{z_j(r_j)} kc_r r\mathrm{d}z\right] \tag{23}$$

where *k* is the blockage factor due to the real blade thickness $(k = z_l\Delta\varphi/2\pi)$.

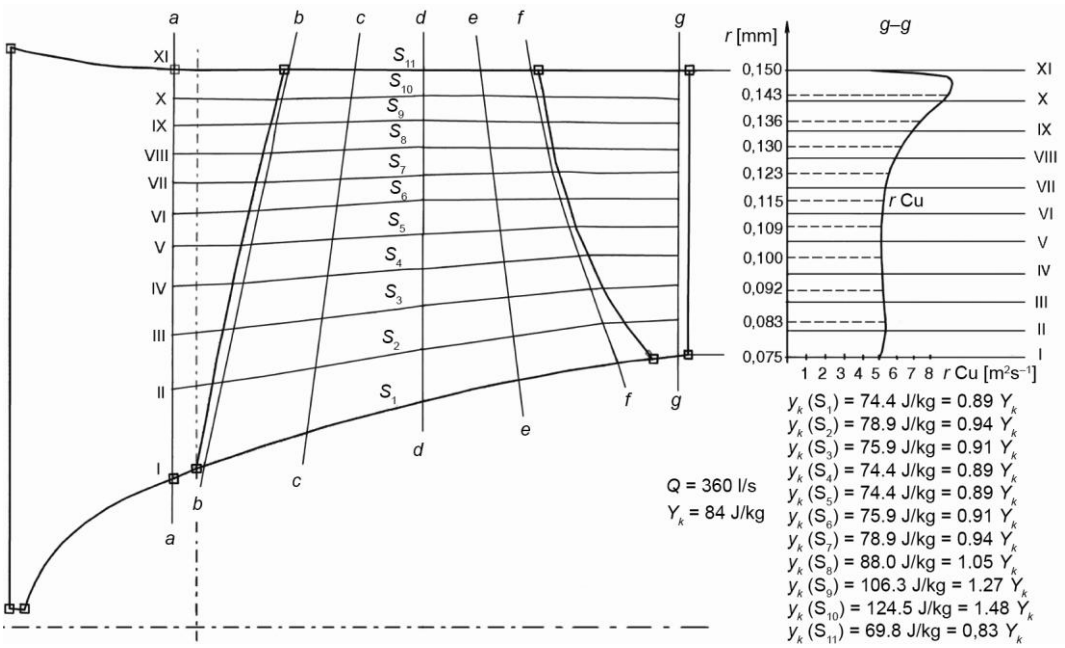

Figure 8. Meridian streamlines of averaged flow and rc_u distribution from hub to tip

In the blade-free flow passages $k = 0$. If j = n, then $Q_l(\mathrm{n}) = Q_l$.

The functional relation between volume flow rate changing along the control meridian line ($Q = Q_l$) can be obtained by calculating the flow rate from one to the other point along the line *l*. If this functional dependence is determined for all control meridian lines, meridian streamlines are determined as the line that passes through all points in control line *l* defining the same flow rate.

If calculating points are placed in high density on control meridian lines, the integral given as eq. (23) can be sufficiently accurately solved using the trapezoidal method.

Meridian streamlines of averaged flow, which are determined for the case of the axial flow pump described in chapter 2 of the paper, are presented in fig. 8.

Numerically obtained results of the flow parameters in the pump impeller were used in the process of averaging, and, as it was mentioned in chapter 2, the ANSYS CFX software was used for that purpose.

For averaging of flow parameters in the pump impeller of investigated four blades pump, seven control meridian lines were used, two of which were in the blade-free area (a-a in front of and g-g behind the blade area), and five control meridian lines were inside the blade area. Eleven points of averaging were uniformly distributed along every meridian control line, and, along the circular arc which passed through these points, ten points (in which flow parameters in the blade passage were numerically obtained) were evenly distributed. The number of points used in the procedure of averaging can be larger than ten, but it was shown that the larger number of points does not significantly influence the obtained results of averaging. Meridian streamlines of averaged flow are denoted with S_2, S_3, … S_{10}, and they are obtained using the integral continuity equation, while S_1 and S_{11} are boundary meridian streamlines (fig. 8).

In the pump inlet, $c_{u1} = 0$, thus the specific work of elementary stage is $y_k(S_j) = \omega(r\bar{c}_u)_g$, where g denotes the outlet meridian cross-section. The diagram of function $(r\bar{c}_u)_g = f(r)$, which is in proportion to the specific works of elementary stages, is also given in fig. 8, showing the unequal distribution of specific work of elementary stages [9, 10].

Conclusions

Using numerical simulations of flow in a designed hydraulic turbomachine, the designer can preliminary estimate the quality of the designed turbomachine, before even the model or prototype of the machine is produced. The numerical simulation itself cannot directly answer two very important questions related to the turbomachinery designing procedure: the designer cannot compare the axisymmetric flow surfaces and the specific work of elementary stages, which were used in the designing procedure of profiling the impeller blades. The answers to these important questions can be given by using the method of averaging of numerically obtained results of flow parameters according to the circular co-ordinate and by determining averaged flow surfaces, obtained using the integral continuity equation. The methodology of the averaging principles and obtained results for one concrete example of axial-flow pump was fully presented in the paper.

The importance of the presented designing procedure lies in saving time and funds during the turbomachinery designing and manufacturing. Last, but not the least, the proper designing of any turbomachinery strongly affects machine energy efficiency and energy efficiency of the system in which this machine is built. Therefore, numerical simulations of flow in designed turbomachinery and determination of averaged axisymmetric flow surfaces were perform in order to obtain better machine efficiency and increase energy efficiency.

Acknowledgments

This paper is a result of the technological project TR33040, “Revitalization of existing and designing new micro and mini hydropower plants (from 100 kW to 1000 kW) in the territory of South and Southeast Serbia”, supported by the Serbian Ministry of Education, Science and Technological Development.

Nomenclature

$\vec{c}$ – absolute velocity [ms^{-1}]
c_m – meridian component of absolute velocity, [ms^{-1}]
c_u – circumferential component of absolute velocity [ms^{-1}]
$\vec{e}_i^o$ – curvilinear orthogonal orts i = 1, 2, 3
$\vec{F}$ – force, [N]
G – Bernoulli's integral for absolute flow, [–]
H – pump head (= Y/g), [m]
k – blockage factor, [–]
L_i – Lamé's coefficients, i = 1, 2, 3
n – rotational speed, [s^{-1}, min^{-1} = rpm]
$\vec{n}$ – unite vector perpendicular to the surface
p – pressure, [Pa]
Q – volume flow rate, [m^{3}s^{-1}]
q_i – curvilinear orthogonal co-ordinate, i = 1, 2, 3
r – radius, [m]
$\vec{u}$ – circumferential velocity, [ms^{-1}]
$\vec{w}$ – realtive velocity, [ms^{-1}]
Y – pump specific work of turbo pump (= $Y_k \cdot \eta_h$), [Jkg^{-1}]
Y_k – specific work of impeller (= $u_2c_{2u} - u_1c_{1u}$) , [Jkg^{-1}]
Y_k – specific work of elementary stage, [Jkg^{-1}]
z_l – number of blades

Greek symbols

$\alpha, \beta, \gamma, \delta$ – angles [°]
η_h – hydraulic efficiency
ψ – stream function [–]
τ – angular blade pitch [–]
ω – angular velocity [rads^{-1}]

Subscripts

a, b – surfaces of the two next blades
g – pressure side of the blade
l – suction side of the blade
m – meridian
sr – average
u – circumferential

References

[1] Babić, M., Stojković S., *Basics of Turbomachinery: Operating Principles and Mathematical Modeling*, University of Kragujevac, Naučna knjiga, Belgrade, 1990
[2] Lakshminarayana, B., *Fluid Dynamics and Heat Transfer of Turbomachinery*, John Wiley & Sons, Inc., New York, USA, 1996
[3] Krsmanović, Lj., Gajić A., *Turbomachinery – Theoretical Basics*, Faculty of Mechanical Engineering, University of Belgrade, Belgrade, 2005
[4] Tanata, S., Hiratani, F., Furukawa, M., Axisymmetric Viscous Flow Modeling for Meridional Flow Calculation in Aerodynamic Design of Half-Ducted Blade Rows, *Memoirs of the Faculty of Engineering, Kyushu University*, *67* (2007), 4, pp. 199-208
[5] Bogdanović-Jovanović, J., Milenković, D., Bogdanović, B., Numerical Simulation of Flow and Operating Characteristics of Axial Flow Pump, *Proceedings*, 32nd Congress HIPNEF 2009,Vrnjačka Banja, Serbia, 2009, pp. 217-224
[6] Casey, M., Best Practice Advice for Turbomachinery Internal Flows, *QNET-CFD Network Newsletter (A Thematic Network For Quality and Trust in the Industrial Application of CFD)*, *2* (2004), 4, pp. 40-46
[7] Ferziger, J. H., Peric, M., *Computational Methods for Fluid Dynamics*, 3rd ed., Springer, 2002
[8] Etinberg, I. E., Rauhman, B. S., *Hydrodynamics of Hydraulic Turbines*, (in Russian), St. Petersburg, Russia, 1978
[9] Bogdanović, B., Bogdanović-Jovanović, J., Spasic, Ž., Designing of Low Pressure Axial Flow Fans with Different Specific Work of Elementary Stages, *Proceedings*, The International Conference Mechanical Engineering in XXI Century, Nis, Serbia, 2010, pp. 99-102
[10] Bogdanović, B., Bogdanović-Jovanović, J., Todorovic, N., Program for Determination of Unequal Specific Work Distribution of Elementary Stages in the Low-Pressure Axial-Flow Fan Design Procedure, *Facta Universitatis, Series: Mechanical Engineering*, *9* (2011), 2, pp. 149-160

Paper submitted: April 26, 2012
Paper revised: June 25, 2012
Paper accepted: July 5, 2012